A Journal of the Gesellschaft Deutscher Chemiker
Angewandte Chemie
International Edition
www.angewandte.org

Title: Maximizing Catalysis of Nanoparticles via Their Monolayer Assembly on Nitrogen-doped Graphene

Authors: Chao Yu, Xuefeng Guo, Mengqi Shen, Bo Shen, Michelle Muzzio, Zhouyang Yin, Qing Li, Zheng Xi, Junrui Li, Christopher Takakazu Seto, and Shouheng Sun

To be cited as: *Angew. Chem. Int. Ed.* 10.1002/anie.201709815
Angew. Chem. 10.1002/ange.201709815

Link to VoR: http://dx.doi.org/10.1002/anie.201709815
http://dx.doi.org/10.1002/ange.201709815

WILEY-VCH

Angewandte Chemie International Edition
10.1002/anie.201709815

Maximizing Catalysis of Nanoparticles via Their Monolayer Assembly on Nitrogen-doped Graphene

Chao Yu†, Xuefeng Guo†, Mengqi Shen, Bo Shen, Michelle Muzzio, Zhouyang Yin, Qing Li, Zheng Xi, Junrui Li, Christopher T. Seto* and Shouheng Sun*

Abstract: We report a facile interface assembly method to assemble a monolayer array of nitrogen-doped graphene (NG) and nanoparticles (NPs) and then to transfer the dual monolayers onto a solid substrate. Using 3 nm NiPd NPs as an example, we demonstrate that NiPd-NG-Si can function as a catalyst probe and show maximum NiPd catalysis for the hydrolysis of ammonia borane (H_3NBH_3, AB) with its TOF = 4896.8 h^{-1} and E_a = 18.8 kJ/mol. The NiPd-NG-Si is also highly active for catalyzing transfer hydrogenation from AB to $-NO_2$, leading to the green chemistry synthesis of quinazolines in water. Our assembly method can be extended to other graphene and NP catalyst materials, providing a new 2D NP catalyst platform for catalyzing multiple reactions in one-pot with maximum efficiency.

The recent push for green chemistry syntheses of functional molecules and materials requires new and efficient catalysts that are able to catalyze multiple chemical reactions. Such catalysts can also serve as models for developing a better understanding of how to design and optimize multifunctional catalysts. One way that this problem has been addressed is to have catalysts arranged in a two-dimensional (2D) array so that each single catalyst unit is exposed to reactants equally for a specific reaction. This is conventionally achieved by using the lithography process in which a catalytically active material is deposited on a pre-patterned substrate.[1] Recently, self-assembly techniques have advanced to a level that functional nanoparticles (NPs) can be deposited on a flat surface[2] and serve as a catalyst layer to achieve higher catalytic activity.[3] However, this approach has been limited to NP deposition on bulk solid surfaces. Efforts to deposit NPs on a flat nanoscale support, such as graphene (G), have met with only limited success for catalytic applications because of difficulties in controlling monodisperse NP deposition on a flat G surface,[2f, 4] or in unfolding the NP-modified G into a flat NP-G array.[5]

Here we report a facile assembly approach to consecutive monolayer assembly of nitrogen-doped G (NG) and NPs to achieve a monolayer NP deposition on NG and further on a flat solid substrate, as outlined in Figure 1. Our assembly strategy is based on liquid/liquid self-assembly of NPs reported as a way for rapid fabrication of 2D nanostructures.[6] By controlling solvent types and solvent evaporation on the water phase, we are able to assemble a monolayer array of NG (Figure 1a), and then a monolayer assembly of NPs (Figure 1b). By lifting a solid substrate (S) from a water phase, we can transfer the monolayer assembly of NPs and NG onto S, giving NPs-NG-S (Figure 1c). The assembly method can be extended to G in general, but pristine G cannot stabilize NPs well enough to survive the NP activation process tested in this paper for catalysis. NG is a better choice for anchoring/stabilizing NPs for catalytic studies due to the N-doping induced disruption of the π-electron cloud on the G surface.[2f, 7] When proper NPs are chosen for the assembly, the NPs-NG-S can serve as a convenient catalyst "probe": Inserting the probe into a solution containing all required reactants will trigger a series of cascade reactions, while pulling the probe away from the solution will stop the reactions (Figure 1c). In this way, we can achieve rational control of reaction kinetics and product formation.

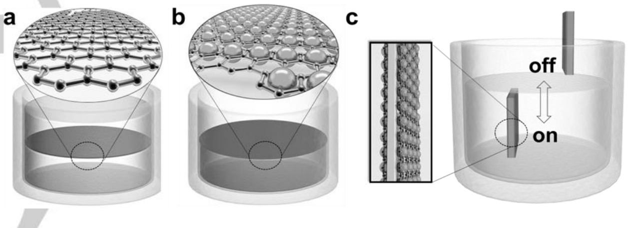

Figure 1. a) Schematic illustration of the interface assembly of monolayer NG. b) Interface assembly of NPs-NG. c) Assembled NPs-NG on both sides of S as a probe to catalyze a solution phase reaction with "on" representing the probe insertion to trigger the catalytic reaction, and "off" indicating the pulling of the probe from the solution to stop the reaction.

We first demonstrate our new strategy to prepare NPs-NG-S. NG was synthesized as reported,[8] and was dispersed in ethanol. Representative NPs of 3 nm $Ni_{30}Pd_{70}$ (denoted as NiPd in this paper),[9] 8 nm Fe_3O_4[10] and 9 nm Pd[11] were also prepared as reported. We modified a previous report on the assembly of graphene oxide (GO) [6b. 12] and performed our assembly by dropping pentane (5 mL) onto a water (5 mL) surface (20 cm^2) to create a pentane-water inter-surface. Then we added 1 mL of ethanol dispersion of NG (0.05 mg/mL) via a syringe into the water phase without disrupting the interface. Evaporation of half of the pentane at room temperature led to formation of a reflective NG film at the interface. When we added 2.5 mL of NP pentane dispersion (0.012 mg/mL) dropwise at this stage and let the pentane completely evaporate, we obtained a monolayer array of NPs directly on the NG film. The film was collected on a SiO-coated Cu grid or a silicon wafer by lifting the substrate up through the water phase, and dried in air. During this process, lifting the substrate at different stages can give us either NG-Si or NPs-NG-Si.

The NG-Si was characterized by atomic force microscope (AFM, Figure 2a, Figure S1). Line scanning across a

---

[*] Dr. C. Yu,[†] X. Guo,[†] M. Shen, B. Shen, M. Muzzio, Z. Yin, Z. Xi, J. Li, Prof. C. T. Seto and Prof. S. Sun
Department of Chemistry, Brown University
Providence, RI, 02912 (United State)
E-mail: christopher_seto@brown.edu
ssun@brown.edu
Prof. Q. Li
School of Materials Science and Engineering, Huazhong University of Science and Technology
Wuhan, Hubei 430074 (China)

[†] These authors contributed equally to this work

Supporting information for this article is given via a link at the end of the document.

representative sheet gave a height profile and film thickness of 0.6 nm, corresponding to the thickness of a single layer of NG.[8, 13] The transmission electron microscope (TEM) images clearly show the monolayer assembly of 3 nm NiPd NPs (Figure 2b), as well as 9 nm Pd and 8 nm Fe_3O_4 NPs (Figure S2&3) on NG. The NP arrays can be further characterized by AFM analysis (Figure 2c). For example, the average thickness of the NiPd-NG is measured to be 3.1 nm. Subtracting the NG thickness of 0.6 nm (Inset of Figure 2a) gives a NP height of 2.5 nm, close to the average NP size measured by TEM, indicating the successfully preparation of a dual-monolayer assembly of NPs and NG (AFM measurements often give smaller dimensions than TEM measurements, especially for NPs with dimensions less than 10 nm due to tip-sample interactions).[14] Under these assembly conditions with a properly controlled NP dispersion concentration, we did not observe NP deposition on the non-NG area of S, indicating that our assembly approach is very selective for the formation of NPs-NG. However, increasing the NP concentration to 0.016 mg/mL or higher caused the NPs to stack in multilayers at the interface (Figure S4a), denoted as $(NiPd)_{>1}$-NG-Si, while reduction of the NP dispersion concentration to 0.008 mg/mL or below resulted in patchy NP assemblies on the NG surface (Figure S4b), denoted as $(NiPd)_{<1}$-NG-Si.

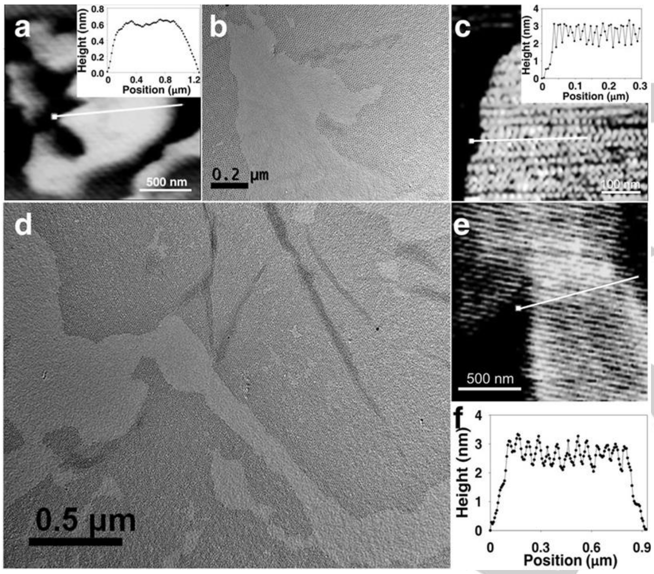

Figure 2. a) AFM image of NG-S (S = Si). Inset: line profile of scanning across the NG. b) TEM image of 3 nm NiPd-NG-S (S = SiO Type-A supported Cu grid). c) AFM image of NiPd-NG-Si. Inset: line profile of scanning across part of the NiPd-NG-Si. d) TEM image of 3 nm NiPd-NG-S (S = SiO Type-A supported Cu grid) annealed at 400 °C. e) AFM image of the annealed NiPd-NG-Si. (f) AFM height profile of line scanning across the annealed NiPd-NG-Si in e).

Monolayer assembly of NPs on NG allows maximum exposure of NPs for catalysis. The NG serves as a Lewis basic support, providing anchoring sites not only for the NPs, but also for Lewis acidic reactants, facilitating the enhancement of NP catalysis.[15] For comparison purposes, we also prepared NiPd-G-Si (Figure S5), as well as physical mixture of NiPd+NG (or G) by mixing NPs and NG (or G) (mass ratio 3/5) in hexane followed by hexane washing. These NPs were activated by annealing in Ar at 400 °C for 2 h. The NiPd-NG-Si shows no NP aggregation (Figure 2d). The AFM image of a representative patch of the annealed sample shows nearly the same height (3.0 nm) when compared to the height measured for a freshly-deposited, unannealed sample (Inset of Figure 2c). However, the NiPd NPs in the NiPd-G-Si structure shows signs of stacking after this annealing treatment (Figure S6). These observations indicate that the NG indeed provides anchoring sites that stabilize the NPs during the NP activation process.

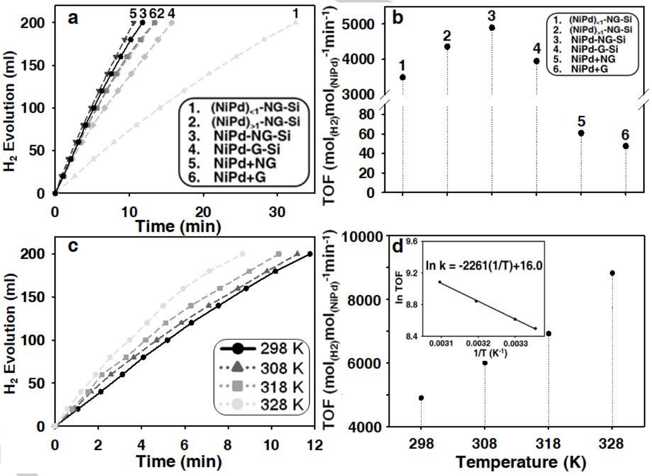

Figure 3. a) Stoichiometric hydrogen evolution from AB hydrolysis catalyzed by NiPd-S prepared via different assembly methods ([AB] = 300 mM, T = 298 K. For NiPd-NG-Si or NiPd-G-Si, [NiPd] = 1.5 ppm and 1.7 ppm, respectively. For $(NiPd)_{<1}$-NG-Si and $(NiPd)_{>1}$-NiPd-NG-Si, [NiPd] = 1.0 ppm and 2.1 ppm, respectively. For NiPd+Support, [NiPd] = 0.15 mg/mL). b) TOF values of NiPd-S prepared via different assembly methods. c) Stoichiometric hydrogen evolution at different temperatures ([AB] = 300 mM, [NiPd] = 1.5 ppm). d) TOF values of NiPd-NG at different temperatures. Inset: Arrhenius plot of ln TOF vs (1/T).

We first tested the assembled NiPd NPs as a catalyst for the hydrolysis of ammonia borane (AB) (the assembled Pd and Fe_3O_4 NPs were much less active than the NiPd NPs). We used the reaction condition that has been optimized for the NiPd NP catalyst (10 mL of 300 mM AB at 298 K)[9] for the comparison purpose, and plotted the data in Figure 3a,b. Compared with other controls, the NiPd-NG-Si catalyst shows much-enhanced activity for AB hydrolysis. $(NiPd)_{>1}$-NG-Si, $(NiPd)_{<1}$-NG-Si and even NiPd-G-Si are all less active than the monolayer assembly NiPd-NG-Si. NiPd + NG (or G) is much less active than the NiPd-NG-Si and requires that the NiPd loading be increased to 0.15 mg/mL for the rate of H_2 production to be comparable with the NiPd-NG-Si (1.5 ppm). These results indicate that 1) monolayer assembly can indeed maximize NiPd catalysis; and 2) the presence of NG enhances the NiPd catalysis due to the NG's role in stabilizing the NiPd NPs and activating NH_3-BH_3 bonding by the NG-BH_3 interaction. The temperature dependence of the catalytic reaction from 298 K-328 K was also measured as shown in Figure 3c. From the slope of the linear plot of ln TOF versus 1/T in Figure 3d, we calculated the activation energy for H_2 evolution from AB to be E_a = 18.8 kJ/mol, and TOF to be 4896.8 mol_{H2} mol_{NiPd}^{-1} min^{-1}. The NiPd-NG-Si has the lowest E_a and highest initial TOF ever reported for AB hydrolysis.[16]

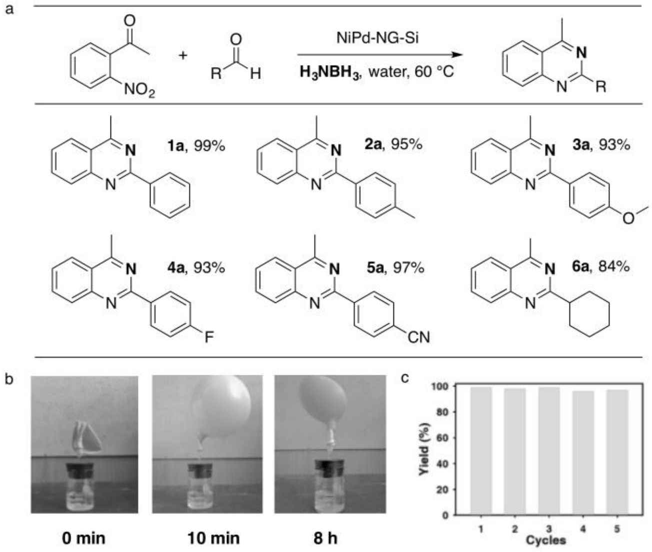

Figure 4. a) Reaction results of 2-nitroacetophenone and various aldehydes. Reaction conditions: 2-nitroacetophenone (1 mmol), aromatic or aliphatic aldehyde (1.2 mmol), NiPd-NG-Si (0.016 mol%), water (20 mL) and AB (3 mmol), 60 °C, 8 h. b) Schematic photos showing the NiPd-NG-catalyzed one-pot synthesis of quinazolines using AB in water. c) Separation yields of quinazoline 1a in successive runs using recycled NiPd-NG-Si).

Since AB hydrolysis has been used directly in transfer hydrogenation reactions for organic reductions,[3b, 17] we explored the advantages of our new catalyst probe for the AB-initiated transfer hydrogenation and for the high-yield synthesis of quinazolines - the key components present in heterocycle compounds for displaying antibacterial, antifungal and anticancer activities.[18] Our NiPd-NG-Si catalyzed the one-pot synthesis of quinazolines from o-nitroacetophenone and benzaldehydes with AB hydrolysis providing the necessary H_2 and NH_3 ($NH_4^+ \rightleftharpoons NH_3 + H^+$) sources, as summarized in Figure 4a. We screened reaction conditions and found that reaction in water at 60 °C for 8 h to be optimal (Table S1 and Table S2). The NiPd-NG-Si was the most active catalyst, giving 4-methyl-2-phenylquinazoline in an excellent yield of 99% in the presence of only 0.016 mol% of NiPd. We tested the NiPd-NG-Si catalyst for similar reactions and found it to be equally active in producing quinazoline derivatives (**1a**-**5a**) regardless of the presence of electron-donating or electron-withdrawing groups on the benzaldehyde. Furthermore, an aliphatic aldehyde, which is much less active under conventional reaction conditions, also reacts well to give **6a** in 84% yield. In the synthesis, we simply inserted the NiPd-NG-Si probe into the solution to initiate the one-pot reaction. From the reaction system photos (Figure 4b), we can see that after the probe is inserted into the reaction solution, the balloon expands quickly due to the fast release of H_2 from AB hydrolysis. As the reaction proceeds, the balloon shrinks due to the consumption of H_2 during the subsequent transfer hydrogenation and other reactions. We can pull the catalyst probe out from the reaction system to stop the reaction and to separate the reaction product. Using the reaction leading to the formation of **1a**, we tested stability of the NiPd-NG-Si catalyst after 5 consecutive reaction runs. In each case, after pulling the catalyst from the reaction solution and washing it with water, the catalyst was ready for the next round of reaction. We found no significant loss of catalytic activity (**1a** yield stayed >95% (Figure 4c) and no obvious change of catalyst morphology (Figure S7), indicating that the NiPd-NG-Si catalyst is not only active, but also stable under the reaction conditions.

We further performed three control experiments (Figure S8) to study the possible reaction mechanism. From control experiment 1, we can see that the reaction without aldehyde gave aromatic amines. The formation of $–NH_2$ and =NH groups shows that the hydrolysis of AB provides both H_2 and NH_3 for the reactions. Control experiment 2 indicates that NH_3 is a reaction component required for the formation of quinazoline. Control experiment 3 confirms that the catalyst is active for dehydro-aromatization, and can further catalyze a second transfer hydrogenation reaction to C=C of styrene. Based on these control experiments and previous reports,[19] we can propose a possible mechanism to explain how the reactions proceed to form the final product (Scheme S1). Overall, compared with previous syntheses of quinazolines,[20] our new catalyst probe shows maximum activity for catalyzing one-pot cascade reactions for the formation of quinazolines in water under mild condition without the addition of any other additives or oxidants.

We have developed a facile interfacial assembly method to prepare a monolayer array of NG and NPs consecutively, and to transfer the NPs-NG onto a solid substrate (S), obtaining the dual NP and NG assemblies on S, NPs-NG-S. This NPs-NG-S can be used as a catalyst probe to turn a catalytic reaction “on” by inserting the probe into the reaction solution and “off” by pulling the probe out of the solution. Using 3 nm NiPd NPs as an example, we have demonstrated that the monolayer NiPd-NG-Si shows the maximum catalysis not only for AB hydrolysis, but also for the following transfer hydrogenation, imine formation, and condensation of aromatic nitro-compounds and aldehydes, leading to the one-pot, high-yield synthesis of quinazolines in water with only 0.016 mol% catalyst loading. Our assembly method can be extended to other G and NPs, providing a new 2D NP platform for catalyzing reactions with optimum efficiency.

Experimental Section

Monolayer Assembly of NPs-NG-S: Pentane (5 mL) was firstly added on the top of water (5 mL) to form a biphasic interface between pentane and water phase. NG was mixed with ethanol (0.05 mg/mL) and 1 mL of this solution was injected into the water phase. Once half of the pentane was evaporated at room temperature, 2.5 mL of NPs/pentane solution (0.012 mg/mL for $Ni_{30}Pd_{70}$, 0.02 mg/mL for Fe_3O_4, 0.02 mg/mL for Pd) was added dropwise to the pentane phase. After pentane evaporation, a large monolayer array was assembled on the surface of the NG, and was then transferred onto S (14 mm x 6 mm silicon wafer or SiO Type-A supported Cu grid) for characterizations. Other experimental details were given in the supporting information.

Acknowledgements

The work was supported by the U.S. Army Research Laboratory and the U.S. Army Research Office under grant W911NF-15-1-0147 (S.S.), by Strem Chemicals (S.S.), by National Natural Science Foundation of China (21603078) and National Materials Genome Project (2016YFB0700600) (Q.L.), as well as by the National Science Foundation Graduate Research Fellowship under Grant No. 1644760 (M.M.).

Keywords: Interfacial assembly • Dual-monolayer • Nanoparticles • Hydrogen Transfer • Heterogeneous catalyst •

[1] a) V. Flauraud, M. Mastrangeli, G. D. Bernasconi, J. Butet, D. T. L. Alexander, E. Shahrabi, O. J. F. Martin, J. Brugger, *Nat. Nanotechnol*. **2017**, *12*, 73-80; b) T. G. W. Edwardson, K. L. Lau, D. Bousmail, C. J. Serpell, H. F. Sleiman, *Nat. Chem*. **2016**, *8*, 162-170; c) S. H. Etschel, L. Portilla, J. Kirschner, M. Drost, F. Tu, H. Marbach, R. R. Tykwinski, M. Halik, *Angew. Chem. Int. Edit*. **2015**, *54*, 9235-9238; d) Y. H. Zheng, C. H. Lalander, T. Thai, S. Dhuey, S. Cabrini, U. Bach, *Angew. Chem. Int. Edit.* **2011**, *50*, 4398-4402; e) J. H. Zhang, Y. F. Li, X. M. Zhang, B. Yang, *Adv. Mater.* **2010**, *22*, 4249-4269; f) K. Q. Peng, Y. Wu, H. Fang, X. Y. Zhong, Y. Xu, J. Zhu, *Angew. Chem. Int. Edit.* **2005**, *44*, 2737-2742; g) V. Santhanam, R. P. Andres, *Nano Lett.* **2004**, *4*, 41-44; h) Y. Cui, M. T. Bjork, J. A. Liddle, C. Sonnichsen, B. Boussert, A. P. Alivisatos, *Nano Lett.* **2004**, *4*, 1093-1098.

[2] a) P. S. Toth, M. Velicky, M. A. Bissett, T. J. A. Slater, N. Savjani, A. K. Rabiu, A. M. Rakowski, J. R. Brent, S. J. Haigh, P. O'Brien, R. A. W. Dryfe, *Adv. Mater.* **2016**, *28*, 8256-8264; b) M. P. Arciniegas, F. Di Stasio, H. B. Li, D. Altamura, L. De Trizio, M. Prato, A. Scarpellini, I. Moreels, R. Krahne, L. Manna, *Adv. Funct. Mater.* **2016**, *26*, 4535-4542; c) P. S. Toth, M. Velicky, Q. M. Ramasse, D. M. Kepaptsoglou, R. A. W. Dryfe, *Adv. Funct. Mater.* **2015**, *25*, 2899-2909; d) L. R. Xu, X. Zhou, W. Q. Tian, T. Gao, Y. F. Zhang, S. B. Lei, Z. F. Liu, *Angew. Chem. Int. Edit.* **2014**, *53*, 9564-9568; e) K. H. Lee, H. J. Shin, B. Kumar, H. S. Kim, J. Lee, R. Bhatia, S. H. Kim, I. Y. Lee, H. S. Lee, G. H. Kim, J. B. Yoo, J. Y. Choi, S. W. Kim, *Angew. Chem. Int. Edit.* **2014**, *53*, 11493-11497; f) Z. L. Li, J. H. Liu, C. G. Xia, F. W. Li, *ACS Catal.* **2013**, *3*, 2440-2448; g) X. Huang, Z. Y. Zeng, S. Y. Bao, M. F. Wang, X. Y. Qi, Z. X. Fan, H. Zhang, *Nat. Commun*. **2013**, *4,* doi:10.1038/ncomms3239; h) A. Reina, X. T. Jia, J. Ho, D. Nezich, H. B. Son, V. Bulovic, M. S. Dresselhaus, J. Kong, *Nano Lett.* **2009**, *9*, 30-35.

[3] a) J. Zhao, Z. Chen, *J. Am. Chem. Soc.* **2017**, *139,* 12480–12487; b) C. Yu, J. J. Fu, M. Muzzio, T. L. Shen, D. Su, J. J. Zhu, S. H. Sun, *Chem. Mater.* **2017**, *29*, 1413-1418; c) Y. Huang, M. Zhao, S. Han, Z. Lai, J. Yang, C. Tan, Q. Ma, Q. Lu, J. Chen, X. Zhang, Z. Zhang, B. Li, B. Chen, Y. Zong, H. Zhang, *Adv. Mater.* **2017**, *29,* doi: 10.1002/adma.201700102; d) D. H. Deng, K. S. Novoselov, Q. Fu, N. F. Zheng, Z. Q. Tian, X. H. Bao, *Nat. Nanotechnol*. **2016**, *11*, 218-230; e) Y. X. Yao, Q. Fu, Y. Y. Zhang, X. F. Weng, H. Li, M. S. Chen, L. Jin, A. Y. Dong, R. T. Mu, P. Jiang, L. Liu, H. Bluhm, Z. Liu, S. B. Zhang, X. H. Bao, *P. Natl. Acad. Sci. USA* **2014**, *111*, 17023-17028; f) X. F. Chen, J. S. Zhang, X. Z. Fu, M. Antonietti, X. C. Wang, *J. Am. Chem. Soc.* **2009**, *131*, 11658-11659.

[4] a) S. C. Xu, B. Y. Man, S. Z. Jiang, J. H. Wang, J. Wei, S. D. Xu, H. P. Liu, S. B. Gao, H. L. Liu, Z. H. Li, H. S. Li, H. W. Qin, *ACS. Appl. Mater. Inter*. **2015**, *7*, 10977-10987; b) Y. Y. Lv, Y. Fang, Z. X. Wu, X. F. Qian, Y. F. Song, R. C. Che, A. M. Asiri, Y. Y. Xia, B. Tu, D. Y. Zhao, *Small*. **2015**, *11*, 1003-1010; c) D. C. Geng, H. P. Wang, G. Yu, *Adv. Mater.* **2015**, *27*, 2821-2837; d) J. W. Liu, R. T. Lu, G. W. Xu, J. Wu, P. Thapa, D. Moore, *Adv. Funct. Mater.* **2013**, *23*, 4941-4948; e) X. Z. Zhou, X. Huang, X. Y. Qi, S. X. Wu, C. Xue, F. Y. C. Boey, Q. Y. Yan, P. Chen, H. Zhang, *J. Phys. Chem. C* **2009**, *113*, 10842-10846.

[5] a) L. H. Wu, J. J. Willis, I. S. McKay, B. T. Diroll, J. Qin, M. Cargnello, C. J. Tassone, *Nature* **2017**, *548*, doi:10.1038/nature23308; b) E. A. Gaulding, B. T. Diroll, E. D. Goodwin, Z. J. Vrtis, C. R. Kagan, C. B. Murray, *Adv. Mater.* **2015**, *27*, 2846-2851; c) A. G. Dong, J. Chen, P. M. Vora, J. M. Kikkawa, C. B. Murray, *Nature* **2010**, *466*, 474-477; d) T. P. Bigioni, X. M. Lin, T. T. Nguyen, E. I. Corwin, T. A. Witten, H. M. Jaeger, *Nat Mater*. **2006**, *5*, 265-270; e) M. Li, H. Schnablegger, S. Mann, *Nature* **1999**, *402*, 393-395.

[6] a) W. Han, Z. Q. Lin, *Angew. Chem. Int. Edit.* **2012**, *51*, 1534-1546; b) F. M. Chen, S. B. Liu, J. M. Shen, L. Wei, A. D. Liu, M. B. Chan-Park, Y. Chen, *Langmuir* **2011**, *27*, 9174-9181; c) S. Biswas, L. T. Drzal, *Nano Lett.* **2009**, *9*, 167-172.

[7] a) Q. Li, W. L. Zhu, J. J. Fu, H. Y. Zhang, G. Wu, S. H. Sun, *Nano Energ.* **2016**, *24*, 1-9; b) B. Li, F. Dai, Q. F. Xiao, L. Yang, J. M. Shen, C. M. Zhang, M. Cai, *Energ. Environ. Sci.* **2016**, *9*, 102-106.

[8] Z. H. Sheng, L. Shao, J. J. Chen, W. J. Bao, F. B. Wang, X. H. Xia, *ACS Nano* **2011**, *5*, 4350-4358.

[9] H. Goksu, S. F. Ho, O. Metin, K. Korkmaz, A. M. Garcia, M. S. Gultekin, S. H. Sun, *ACS Catal.* **2014**, *4*, 1777-1782.

[10] P. X. Xi, K. Cheng, X. L. Sun, Z. Z. Zeng, S. H. Sun, *Chem. Commun.* **2012**, *48*, 2952-2954.

[11] G. M. Jiang, H. Y. Zhu, X. Zhang, B. Shen, L. H. Wu, S. Zhang, G. Lu, Z. B. Wu, S. H. Sun, *ACS Nano* **2015**, *9*, 11014-11022.

[12] Y. P. Wang, H. L. Fu, Q. W. Huang, Y. Cui, Y. Sun, L. H. Jiang, *Energy* **2015**, *93*, 854-863.

[13] C. Y. He, Z. S. Li, M. L. Cai, M. Cai, J. Q. Wang, Z. Q. Tian, X. Zhang, P. K. Shen, *J. Mater. Chem. A* **2013**, *1*, 1401-1406.

[14] a) M. Cargnello, N. L. Wieder, T. Montini, R. J. Gorte, P. Fornasiero, *J. Am. Chem. Soc.* **2010**, *132*, 1402-1409; b) A. Mechler, J. Kopniczky, J. Kokavecz, A. Hoel, C. G. Granqvist, P. Heszler, *Phys. Rev. B* **2005**, *72,* doi: 10.1103/PhysRevB.72.125407; c) Y. Ebenstein, E. Nahum, U. Banin, *Nano Lett.* **2002**, *2*, 945-950.

[15] a) X. J. Cui, Y. H. Li, S. Bachmann, M. Scalone, A. E. Surkus, K. Junge, C. Topf, M. Beller, *J. Am. Chem. Soc.* **2016**, *138*, 457-457; b) Q. Y. Bi, J. D. Lin, Y. M. Liu, H. Y. He, F. Q. Huang, Y. Cao, *Angew. Chem. Int. Edit.* **2016**, *55*, 11849-11853; c) F. Chen, A. E. Surkus, L. He, M. M. Pohl, J. Radnik, C. Topf, K. Junge, M. Beller, *J. Am. Chem. Soc.* **2015**, *137*, 11718-11724; d) Y. Zheng, Y. Jiao, L. Ge, M. Jaroniec, S. Z. Qiao, *Angew. Chem. Int. Edit.* **2013**, *52*, 3110-3116.

[16] a) W. W. Zhan, Q. L. Zhu, Q. Xu, *ACS Catal.* **2016**, *6*, 6892–6905. b) A. Rossin, M. Peruzzini. *Chem. Rev.* **2016**, *116*, 8848–8872.

[17] a) Z. H. Shao, S. M. Fu, M. F. Wei, S. L. Zhou, Q. Liu, *Angew. Chem. Int. Edit.* **2016**, *55*, 14653-14657; b) S. Rej, C. F. Hsia, T. Y. Chen, F. C. Lin, J. S. Huang, M. H. Huang, *Angew. Chem. Int. Edit.* **2016**, *55*, 7222-7226; c) H. C. Brown, J. Chandrasekharan, *J. Am. Chem. Soc.* **1984**, *106*, 1863-1865; d) G. E. Ryschkewitsch, *J. Am. Chem. Soc.* **1960**, *82*, 3290-3294.

[18] a) V. Colotta, D. Catarzi, F. Varano, O. Lenzi, G. Filacchioni, C. Costagli, A. Galli, C. Ghelardini, N. Galeotti, P. Gratteri, J. Sgrignani, F. Deflorian, S. Moro, *J. Med. Chem.* **2006**, *49*, 6015-6026; b) Z. Z. Ma, Y. Hano, T. Nomura, *Heterocycles* **2005**, *65*, 2203-2219; c) P. A. Ple, T. P. Green, L. F. Hennequin, J. Curwen, M. Fennell, J. Allen, C. Lambert-van der Brempt, G. Costello, *J. Med. Chem.* **2004**, *47*, 871-887.

[19] a) C. Yu, X. F. Guo, Z. Xi, M. Muzzio, Z. Y. Yin, B. Shen, J. R. Li, C. T. Seto, S. H. Sun, *J. Am. Chem. Soc.* **2017**, *139*, 5712-5715; b) L. Tang, X. H. Zhao, G. D. Zou, Y. Q. Zhou, X. K. Yang, *Asian J. Org. Chem.* **2016**, *5*, 335-339; c) L. Tang, Y. Yang, L. X. Wen, S. Zhang, Z. G. Zha, Z. Y. Wang, *Org. Chem. Front.* **2015**, *2*, 114-118; d) L. Tang, X. F. Guo, Y. Yang, Z. G. Zha, Z. Y. Wang, *Chem. Commun.* **2014**, *50*, 6145-6148.

[20] a) Z. Y. Chen, J. X. Chen, M. C. Liu, J. C. Ding, W. X. Gao, X. B. Huang, H. Y. Wu, *J. Org. Chem.* **2013**, *78*, 11342-11348; b) Y. Z. Yan, Y. H. Zhang, C. T. Feng, Z. G. Zha, Z. Y. Wang, *Angew. Chem. Int. Edit.* **2012**, *51*, 8077-8081; c) X. W. Liu, H. Fu, Y. Y. Jiang, Y. F. Zhao, *Angew. Chem. Int. Edit.* **2009**, *48*, 348-351; d) J. R. Li, X. Chen, D. X. Shi, S. L. Ma, Q. Li, Q. Zhang, J. H. Tang, *Org. Lett.* **2009**, *11*, 1193-1196.

10.1002/anie.201709815

COMMUNICATION

A simple interfacial assembly method was developed to assemble a monolayer of nanoparticles and nitrogen-doped graphene (NG) onto a solid substrate. The as-prepared NiPd-NG-Si serves as a robust and highly efficient catalyst probe for the hydrolysis of ammonia borane and for the following up tandem reactions that lead to the high yield synthesis of quinazolines in water.

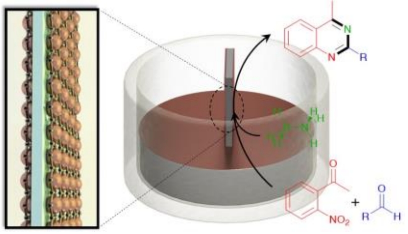

Chao Yu†*, Xuefeng Guo*†*, Mengqi Shen, Bo Shen, Michelle Muzzio, Zhouyang Yin, Qing Li, Zheng Xi, Junrui Li, Christopher T. Seto* and Shouheng Sun**

Page No. – Page No.

Maximizing Catalysis of Nanoparticles via Their Monolayer Assembly on Nitrogen-doped Graphene